Advances in Materials Research, *Vol. 12, No. 2 (2023) 161-177*
https://doi.org/10.12989/amr.2023.12.2.161

Free vibration of functionally graded carbon nanotubes reinforced composite nanobeams

Miloud Ladmek[1], Abdelkader Belkacem[1], Ahmed Amine Daikh[1,2], Aicha Bessaim[1], Aman Garg[3,4], Mohammed Sid Ahmed Houari*[1], Mohamed-Ouejdi Belarbi[5] and Abdelhak Ouldyerou[6,7]

[1]*Laboratoire d'Etude des Structures et de Mécanique des Matériaux, Département de Génie Civil, Faculté des Sciences et de la Technologie, Université Mustapha Stambouli, B.P. 305, R.P., Mascara 29000, Algeria*
[2]*Department of Technology, University Centre of Naama, Naama 45000, Algeria*
[3]*Department of Civil Engineering, National Institute of Technology, Kurukshetra, Haryana 136119, India*
[4]*Department of Aerospace Engineering, Indian Institute of Technology, Kanpur, Uttar Pradesh 208016, India*
[5]*Laboratoire de Recherche en Génie Civil, LRGC, Université de Biskra, B.P. 145, R.P. 07000, Biskra, Algeria*
[6]*Department of Engineering Management, College of Engineering, Prince Sultan University, Riyadh, 11586, Saudi Arabia*
[7]*Department of Mechanical Engineering, Faculty of Science and Technology, University of Mascara, Mascara, Algeria*

(Received December 29, 2022, Revised March 2, 2023, Accepted March 3, 2023)

Abstract. This paper proposes an analytical method to investigate the free vibration behaviour of new functionally graded (FG) carbon nanotubes reinforced composite beams based on a higher-order shear deformation theory. Cosine functions represent the material gradation and material properties via the thickness. The kinematic relations of the beam are proposed according to trigonometric functions. The equilibrium equations are obtained using the virtual work principle and solved using Navier's method. A comparative evaluation of results against predictions from literature demonstrates the accuracy of the proposed analytical model. Moreover, a detailed parametric analysis checks for the sensitivity of the vibration response of FG nanobeams to nonlocal length scale, strain gradient microstructure-scale, material distribution and geometry.

Keywords: higher order nonlocal strain gradient theory; nanobeams; Navier's solution; novel trigonometric FGM; vibration

1. Introduction

Nowadays, carbon nanotubes (CNTs) are being proposed as the most candidates for composite reinforcement material due to their remarkable mechanical, electrical, and thermal properties. These properties include a high tensile modulus, high strength, low density, good conductivity, and

*Corresponding author, Professor, E-mail: ms.houari@univ-mascara.dz

http://www.techno-press.org/?journal=amr&subpage=5 ISSN: 2234-0912 (Print), 2234-179X (Online)

the ability to sustain sizeable elastic strain (Jam and Kiani 2015, Esen and Özmen 2022a). Occasionally, distinct gradation functions may grade CNTs along a particular path rather than dispersing them evenly. They are known as functionally graded CNTs reinforced composites in this instance (FG-CNTRC). Thus, the FG-CNTRCs are the composites in which the pattern the CNTs are embedded in the polymer follows a specific gradation pattern. Because of the gradation of CNTs, the stiffness in the desired direction can be controlled as per the choice of the designer or engineer. This is similar to the case for the functionally graded materials in which the material property varies along the desired direction in a regular fashion (Bessaim *et al.* 2015, Houari *et al.* 2018, Merzouki *et al.* 2022, Esen *et al.* 2021, 2022). Liew *et al.* (2015) performed a comprehensive study on the analysis of FG-CNTRC constructs subjected to various mechanical loads. The constructions were tested under a variety of conditions. Recently, Garg *et al.* (2021) conducted a comprehensive literature assessment discussing the predictions of material properties for single-walled CNTs. Keleshteri *et al.* (2019) investigated the nonlinear bending behavior of FG-CNTRC annular plates with an irregular thickness on elastic foundation plates employing the third-order shear deformation theory. Yas and Samadi (2012) investigated the free vibrations and buckling responses of FG-CNTRC Timoshenko beams with the generalized differential quadrature method (GDQM). Mirzaei and Kiani (2015, 2016), Kiani (2015), Kiani and Mirzaei (2019) employed Ritz method-based FSDT for studying the snap-through and free vibration behavior of sandwich beams containing FG-CNTRC face sheets subjected to thermal conditions. Khosravi *et al.* (2019a, b) carried out buckling and free vibration analysis of rotating FG-CNTRC beams under thermal conditions using differential quadrature method employed in the framework of FSDT. With the help of different beam theories, Babaei *et al.* (2021a, b) predicted the vibration behavior of FG-CNTRC beams resting on elastic foundations. With the help of scale-dependent models, the dynamics of finite element-based Timoshenko beam under the influence of the magnetic field and moving loads were studied by Esen (2020) and Alazwari *et al.* (2020). Zghal *et al.* (2020) utilised an isoparametric finite shell element to perform a nonlinear large deflection investigation on FG-CNTRC plates and panels based on FSDT.

Free vibration analysis of size dependent FG nanoplates was carried out by Esen and Ozmen (2022b). Ozmen *et al.* (2022) predicted the dynamic behavior of scale-based beams under magnetic and thermal fields. El-Ashmawy and Xu (2021) used a two-node finite element (FE) analysis based on TBT to integrate the function of CNTs distribution and orientation on FG nanocomposite beams. Lin and Xiang (2014a, b) used the polynomial Ritz method to investigate the free-vibration properties of FG-CNTRC beams with soft-clamped and hard-clamped boundary conditions based on first-order and third-order shear deformation theories. In order to study the free vibration analysis of FG-CNTRC structures of revolution, including spherical panels and doubly curved shells, Wang *et al.* (2018) proposed a unified semi-analytical technique based on the differential quadrature method and the Mindlin plate theory. By combining the FSDT and the finite element technique. The static and free vibration responses of FG-CNT plates were investigated by Zhu *et al.* (2012). The nonlinear stability of sandwich beams with FG-CNTRC face sheets under thermal loading and a two-parameter elastic foundation was studied by Kiani and Mirzaei (2019) based on the TBT. The free vibration and buckling of FG-CNTRC beams with various thicknesses resting on elastic foundations were also examined by Mohseni and Shakouri (2019). Talebizadehsardari *et al.* (2020) investigated the static bending behavior of the FG-CNTRC curved nanobeam based on TBT. A comparison study analyzing the applicability of various analytical shear deformation theories for the bending, free vibration, and buckling analysis of CNTRC beams was conducted by Wattanasakulpong and Ungbhakorn (2013) inside the framework of HSDTs.

Later, Mayandi and Jeyaraj (2015) studied the linear vibration behavior of FG-CNTRC beams using FSDT and third-order shear deformation theory (TSDT), and the bending and buckling behavior of FG-CNTRC beams under non-uniform thermal loading. Khelifa *et al.* (2018) utilised the sinusoidal shear deformation theory (SSDT) to analyse the buckling response of the FG-CNTRC beam standing on an elastic foundation with consideration for the influence of stretching. Daikh *et al.* (2020) proposed a new hyperbolic shear deformation theory to study the static behaviour of supported cross-ply CNTs-reinforced composite laminated nanobeams under various loading profiles. Using an exponential shear deformation theory, Keshtegar *et al.* (2016) studied the dynamic stability characteristics of a hybrid nanocomposite polymer beam reinforced by CNTs. The authors derived the governing equations using DQM and Bolotin methods. Based on extended high-order panel theory, Salami (2018) studied the bending and free vibration responses of a sandwich beam with a soft core and FG-CNTRC face sheets. The thermo-elastic behavior of FG-CNTRC cross-ply laminated plates under temperature loading was recently analyzed by Bachiri *et al.* (2021) using a novel HSDT. Based on the TSDT, Abdelrahman *et al.* (2022) executed a dynamic analysis of a FG-CNTRC nanobeam resting on an elastic base under a moving load. Using quasi-3D nonlocal strain gradient theory, Daikh *et al.* (2022) presented a comprehensive study on the free vibration, static stability, and bending of multilayer FG-CNTRC nanoplates. Later, Garg *et al.* (2020) used finite elements based on higher-order zigzag theory to analyze the bending and free vibration of FG-CNTR sandwich beams. The authors have assumed that the two face sheets are made of FG-CNTRC and that the core is composed of balsa wood.

In this study, the free vibrations of composite beams reinforced with carbon nanotubes are analyzed using a novel method of material distribution. The present work investigates the free vibrations of (CNTs) reinforced composite beams by considering a new type of material distribution. In this, numerical results are presented and thoroughly explained by considering the impacts of thickness ratio, material distribution, and nonlocal and length scale characteristics on the vibrational behaviour of (CNTRC) beams.

2. Modeling of CNTRC beams

To start with, as is represented in Fig. 1, an uniform CNTRC beam of length L, and thickness h is taken into consideration. Therefore, each lamina of the beam is reinforced by SWCNTs according to different distributions of gradation function which is also represented in Fig. 1(b). The used CNTs distribution patterns are in function of the volume fraction of CNTs *Vcnt* as

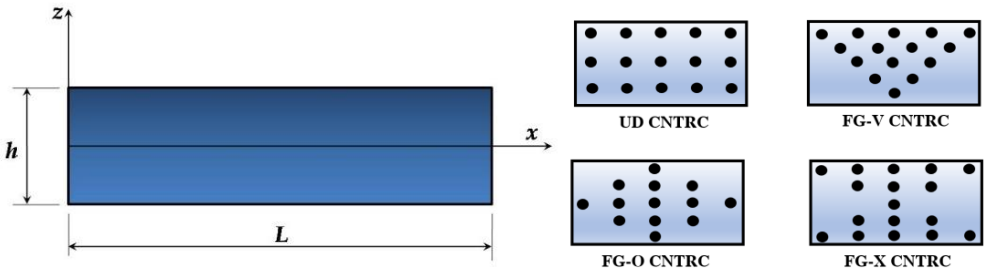

Fig. 1 Geometry and cross-sections of FG-CNTRC beam

$$V_{cnt} = \begin{cases} V_{cnt}^{*} & \text{UD CNTRC} \quad (1) \\ 4\dfrac{|z|}{h}V_{cnt}^{*} & \text{FG-X CNTRC} \quad (2) \\ 2\left(1-\dfrac{2|z|}{h}\right)V_{cnt}^{*} & \text{FG-O CNTRC} \quad (3) \\ \left(1-\dfrac{2z}{h}\right)V_{cnt}^{*} & \text{FG-V CNTRC} \quad (4) \end{cases}$$

Moreover, the UD CNTRC indicate the uniform distribution, whereas, FG-V, FG-O and FG-X present the non-uniform functionally graded distributions. *z*(*k*) and are the vertical positions of the bottom of the beam. *V*cnt* Denote the given volume fraction of CNTs. For the trigonometric FGP-A plate type A, Young's modulus is given as

$$V_{cnt} = \left(1-\cos\left(N\frac{2\pi z}{h}\right)\right)V_{cnt}^{*} \quad (5)$$

For the trigonometric FGP-B plate type B, Young's modulus is given as

$$\mathrm{V_{cnt}} = \left(1+\cos\left(\mathrm{N}\frac{2\pi z}{\mathrm{h}}\right)\right)\mathrm{V_{cnt}^{*}} \quad (6)$$

Wcnt, *ρcnt* and *ρm* are the CNTs mass fraction, CNTs mass density and polymer matrix mass density, respectively.

The effective Young's modulus (*E*) and shear modulus (*G*) of a CNTRC sheet are given as

$$E_{11} = \eta_1 V_{cnt} E_{11}^{cnt} + V_p E^p \quad (7a)$$

$$\frac{\eta_2}{E_{22}} = \frac{V_{cnt}}{E_{22}^{cnt}} + \frac{V_p}{E^p} \quad (7b)$$

$$\frac{\eta_3}{G_{12}} = \frac{V_{cnt}}{G_{12}^{cnt}} + \frac{V_p}{G^p} \quad (7c)$$

Poisson's ratio ν_{12} and density ρ of each sheet can be expressed as

$$\nu_{12} = V_{cnt}{\nu_{12}}^{cnt} + V_p \nu^p \quad (8)$$

$$\rho = V_{cnt}\rho^{cnt} + V_p\rho^p \quad (9)$$

Where $\mathrm{E_{11}}$ and E_{22} are Young's modulus across the plane directions (*x*,*z*), and $\mathrm{G_{12}}$ is the shear modulus of the plate composites. ρandνare the mass density and Poisons coefficient, respectively. The superscriptsp and cnt refer to the mechanical characteristics of the polymer and the SWCNTs, respectively. The CNT efficiency parameters $\eta_i (i = 1,2,3)$ are:

Table 1 The CNTs efficiency parameters

V_{cnt}^{*}	η_1	η_2	η_3
0.12	1.2833	1.0556	1.0556
0.17	1.3414	1.7101	1.7101
0.28	1.3238	1.7380	1.7380

The parameters η_i $(i = 1,2,3)$ are the CNTs efficiency parameters.

3. Equilibrium equations

A quasi-2D parabolic shear deformation beam theory for FG nanobeam considering transverse shear deformations is adopted in this study. The displacement field of the proposed theory is chosen based on the following assumptions (Daikh *et al.* 2020):

(1) The axial displacement consists of extension, bending and shear components;

(2) The bending component of axial displacement is similar to that given by the Euler-Bernoulli beam theory;

(3) The shear component of axial displacement gives rise to the parabolic variation of shear strain and hence to shear stress through the thickness of the beam in such a way that shear stress vanishes on the top and bottom surfaces.

Based on the assumptions made above, the displacement field of the present theory can be obtained as

$$u(x,z,t) = u_0(x,t) - z\frac{\partial w}{\partial x} + f(z)\phi_x(x,t)$$
$$w(x,z,t) = w_0(x,t) \tag{10}$$

where u_0 is the axial displacement; w_0 is the transverse displacement of a mid-line point of the beam; ϕ_x is the rotation of a cross section of the beam at the neutral axis due to transverse shear deformation.

In the current study, the shear deformation along the thickness direction can be expressed by a hyperbolic function in the form

$$f(z) = 5h\tan\left(\frac{z}{h}\right) - 4z \tag{11}$$

The kinematic strain components associated with the displacements are stated as

$$\varepsilon_{xx} = \varepsilon_{xx}^{(0)} + z\varepsilon_{xx}^{(1)} + f(z)\varepsilon_{xx}^{(2)}$$
$$\gamma_{xz} = g(z)\gamma_{xz}^{(0)} \tag{12}$$

where

$$\varepsilon_{xx}^{(0)} = \frac{\partial u_0}{\partial x}, \varepsilon_{xx}^{(1)} = \frac{\partial^2 w_0}{\partial x^2}, \varepsilon_{xx}^{(2)} = \frac{\partial \phi_x}{\partial x}, \gamma_{xz}^{(0)} = \phi_x \tag{13a}$$

The function $g(z)$ is given as follows:

$$g(z) = f'(z) \tag{13b}$$

To obtain the equations of motion, Hamilton's principle is employed as the following

$$\int_{t_1}^{t_2}(\delta U - \delta K)dt = 0 \tag{14}$$

To start with,$\delta U$is the total strain energy, and $\delta K$is the kinetic energy. Therefore, the virtual strain energy of the beam can be expressed as

$$\delta U = \int_0^L \int_{-h/2}^{h/2}(\delta\varepsilon^T\sigma)\,dxdz \tag{15}$$

$$\delta U = \int_0^L \left(N_x \frac{\partial \delta u_0}{\partial x} - M_x \frac{\partial \delta \phi_0}{\partial x} - P_x \frac{\partial^2 \delta w_0}{\partial x^2} + Q_{xz} \delta \phi_x \right) dx + \left[N_x^{(1)} \frac{\partial \delta u_0}{\partial x} - M_x^{(1)} \frac{\partial \delta \phi_0}{\partial x} - P_x^{(1)} \frac{\partial^2 \delta w_0}{\partial x^2} + Q_{xz}^{(1)} \delta \phi_x \right]_0^L \tag{16}$$

where N_x, M_x, P_x and Q_{xz} are, respectively, the axial force, bending moment, shear moment, and shear force. They are defined by

$$(N_x, M_x, P_x) = b \int_{-h/2}^{h/2} (1, z, f(z))\, \sigma_x dz \tag{17a}$$

$$Q_{xz} = b \int_{-h/2}^{h/2} g(z) \tau_{xz} dz \tag{17b}$$

The kinetic energy δK can be written as the following

$$\delta K = b \int_0^L \rho(z) (\dot{u} \delta \dot{u} + \dot{w} \delta \dot{w})\, dx \tag{18a}$$

$$\delta K = b \int_0^L \rho(z) \begin{bmatrix} (I_0 \ddot{u}_0 \delta \dot{u}_0) - I_1 \frac{\partial \dot{w}_0}{\partial x} + I_2 \left(\frac{\partial \dot{w}_0}{\partial x} \frac{\partial \delta \dot{w}_0}{\partial x} \right) \\ + I_3 \left(\frac{\partial \dot{w}_0}{\partial x} \delta \dot{u}_0 - \dot{\phi}_0 \delta \dot{u}_0 + \dot{u}_0 \frac{\partial \delta \dot{w}_0}{\partial x} - \dot{u}_0 \delta \dot{\phi}_0 \right) \\ + I_4 \left(\frac{\partial \delta \dot{w}_0}{\partial x} \delta \dot{u}_0 - 2 \frac{\partial \dot{w}_0}{\partial x} \frac{\partial \delta \dot{w}_0}{\partial x} + \frac{\partial \dot{w}_0}{\partial x} \delta \dot{\phi}_0 \right) \\ + I_5 \left(\frac{\partial \dot{w}_0}{\partial x} \frac{\partial \delta \dot{w}_0}{\partial x} - \dot{\phi}_0 \frac{\partial \delta \dot{w}_0}{\partial x} - \frac{\partial \dot{w}_0}{\partial x} \delta \dot{\phi}_0 + \dot{\phi}_0 \delta \dot{\phi}_0 \right) \end{bmatrix} dx \tag{18b}$$

The mass moments of inertia I_i $(i = 0,1,2, \cdots 5)$ can be defined as

$$(I_0, I_1, I_2, I_3, I_4, I_5) = \int_{-h/2}^{h/2} \rho(z) (1, z, z^2, f(z), z\, f(z), f^2(z))\, dz \tag{19}$$

Moreover, by substituting the equations of δU and δK into Eq.(14), and by applying the integration-by-parts and collecting the coefficients of δu_0, δw_0 and $\delta \phi_0$, it leads to the following equations of motion.

$$\delta\, u_0 : \quad \frac{\partial N_x}{\partial x} = I_0 \ddot{u}_0 - I_1 \frac{\partial \ddot{w}_0}{\partial x} + I_3 \left(\frac{\partial \ddot{w}_0}{\partial x} - \ddot{\phi}_0 \right) \tag{20a}$$

$$\delta\, w_0 : \frac{\partial^2 M_x}{\partial x^2} - \frac{\partial^2 P_x}{\partial x^2} + \frac{\partial Q_x}{\partial x} = I_0 \ddot{w}_0 + I_1 \frac{\partial \ddot{u}_0}{\partial x} - I_2 \nabla^2 \ddot{w}_0 + I_3 \frac{\partial \ddot{u}_0}{\partial x} + I_4 \left(\frac{\partial \ddot{\phi}_0}{\partial x} - 2 \frac{\partial^2 \ddot{w}}{\partial x^2} \right) + I_5 \left(\frac{\partial^2 \ddot{w}}{\partial x^2} - \frac{\partial \ddot{\phi}_0}{\partial x} \right) \tag{20b}$$

$$\delta\, \phi_0 : \quad \frac{\partial P_x}{\partial x} - Q_x = I_3 \ddot{u}_0 - I_4 \frac{\partial \ddot{w}_0}{\partial x} + I_5 \left(\frac{\partial \ddot{w}_0}{\partial x} - \ddot{\phi}_0 \right) \tag{20c}$$

The associated boundary conditions at $x = 0$ and $x = L$ are given as follows:

$$N_x = 0 \text{ or } u = 0$$
$$M_x = 0 \text{ or } w = 0$$
$$\frac{\partial M_x}{\partial x} - \frac{\partial\ P_x}{\partial x} + Q_x = 0 \text{ or } w = 0 \text{ or } w = 0$$

As it is observed, the Eq. (20) are the function of stress resultants. However, the normal and shear stresses by utilizing the constitutive relations can be expressed as

$$\begin{Bmatrix} \sigma_{xx} \\ \sigma_{xz} \end{Bmatrix} = \begin{bmatrix} Q_{11} & 0 \\ 0 & Q_{55} \end{bmatrix} \begin{Bmatrix} \varepsilon_{xx} \\ \gamma_{xz} \end{Bmatrix} \tag{21}$$

Where σ_{xx} and σ_{xz} are the axial and transverse shear stresses. Q_{ij} are the stiffness coefficients correlated with the engineering constants as follows

$$Q_{11} = \frac{E_{11}(z)}{1-\nu^2(z)} \text{ and } Q_{55} = G_{12}(z) \tag{22}$$

Substituting Eqs. (12) and (13) into Eq. (21), and using (17), one the obtains stress resultants

$$\begin{gathered} N_{xx} = A_{11}\varepsilon_x^0 + B_{11}\varepsilon_x^1 + C_{11}\varepsilon_x^2 \\ M_{xx} = B_{11}\varepsilon_x^0 + D_{11}\varepsilon_x^1 + F_{11}\varepsilon_x^2 \\ P_{xx} = C_{11}\varepsilon_x^0 + F_{11}\varepsilon_x^1 + H_{11}\varepsilon_x^2 \\ Q_{xz} = A_{55}\gamma_{xz} \end{gathered} \tag{23}$$

where the cross-sectional rigidities are expressed as

$$(A_{11}, B_{11}, D_{11}, C_{11}, F_{11}, H_{11}) = \int_{-h/2}^{h/2} Q_{11}(1, z, z^2, f(z), z\,f(z), f(z)^2)dz \tag{24}$$

$$A_{55} = \int_{-h/2}^{h/2} Q_{55} g(z)^2 dz \tag{25}$$

The force and moment resultants can be defined in displacement fields as follows

$$\begin{gathered} N_{xx} = A_{11}\frac{\partial u_0}{\partial x} - B_{11}\frac{\partial^2 w_0}{\partial x^2} + C_{11}\left(\frac{\partial^2 w_0}{\partial x^2} - \frac{\partial\ \phi_0}{\partial x}\right) \\ M_{xx} = B_{11}\frac{\partial u_0}{\partial x} - D_{11}\frac{\partial^2 w_0}{\partial x^2} + F_{11}\left(\frac{\partial^2 w_0}{\partial x^2} - \frac{\partial\ \phi_0}{\partial x}\right) \\ P_{xx} = C_{11}\frac{\partial u_0}{\partial x} - F_{11}\frac{\partial^2 w_0}{\partial x^2} + H_{11}\left(\frac{\partial^2 w_0}{\partial x^2} - \frac{\partial\ \phi_0}{\partial x}\right) \\ Q_{xz} = A_{55}\left(\frac{\partial\ w_0}{\partial x} - \phi_0\right) \end{gathered} \tag{26}$$

4. Nonlocal strain gradient theory

By the coupling physical impact of the strain gradient stress and nonlocal elastic stress fields, Lim *et al.* (2015) proposed a function of stresses as

$$\sigma_{ij} = \sigma_{ij}^{(0)} - \frac{\partial \sigma_{ij}^{(1)}}{\partial x} \tag{27}$$

Where $\sigma_{ij}^{(0)}$ and $\sigma_{ij}^{(1)}$ are the classical stress corresponds to strain ε_{kl} and the higher-order stress $\sigma_{ij}^{(1)}$ corresponds to strain gradient $\varepsilon_{kl,x}$ respectively, and can be expressed as

$$\sigma_{ij}^{(0)} = \int_0^L C_{ijkl}\,\alpha_0(x, x', e_0 a)\varepsilon_{kl,x}(x')dx \tag{28a}$$

$$\sigma_{ij}^{(1)} = l^2 \int_0^L C_{ijkl}\,\alpha_1(x, x', e_1 a)\varepsilon_{kl,x}(x')dx \tag{28b}$$

C_{ijkl} denote an elastic constant and l is the material length scale parameter introduced to consider the importance of the strain gradient stress field. Moreover, e_0a and e_1a are the nonlocal parameters introduced to treat the importance of the nonlocal elastic stress field.

The nonlocal kernel functions $\alpha_0(x,x',e_0a)$ and $\alpha_1(x,x',e_1a)$ satisfy the developed conditions by Eringen (1983), The general constitutive relation become as

$$[1-(e_1a)^2\nabla^2]\,[1-(e_0a)^2\nabla^2]\sigma_{ij}=C_{ijkl}[1-(e_1a)^2\nabla^2]\varepsilon_{kl}-C_{ijkl}l^2[1-(e_0a)^2\nabla^2]\nabla^2\varepsilon_{kl} \quad (29)$$

∇^2 is the Laplacian operator.

In the current work, we suppose the coefficient $e=e_0=e_1$. The total nonlocal strain gradient constitutive relation can be stated as

$$[1\text{-}\mu\nabla^2]\sigma_{ij}=C_{ijkl}[1\text{-}\lambda\nabla^2]\varepsilon_{kl} \quad (30)$$

where $\mu=(ea)^2$and $\lambda=l^2$.

$$(1-(e_0a)^2\nabla^2)\sigma_{ij}=C_{ijkl}(1-l^2\nabla^2)\varepsilon_{kl} \quad (31)$$

Therefore, the constitutive relations can be expressed as

$$\sigma_{xx}\text{-}\mu\frac{\partial^2\sigma_{xx}}{\partial x^2}=Q_{11}\left(\varepsilon_{xx}\text{-}\lambda\frac{\partial^2\varepsilon_{xx}}{\partial x^2}\right) \quad (32)$$

$$\sigma_{xz}\text{-}\mu\frac{\partial^2\sigma_{xz}}{\partial x^2}=Q_{55}\left(\gamma_{xz}\text{-}\lambda\frac{\partial^2\gamma_{xz}}{\partial x^2}\right) \quad (33)$$

To obtain the equations of motion in the form of displacements, the stress resultants presented in Eq. (26) are substituted into Eq. (20)

$$N_{xx}-\mu\frac{\partial^2N_{xx}}{\partial x^2}=\left(1-\lambda\frac{\partial^2}{\partial x^2}\right)\left[A_{11}\frac{\partial u_0}{\partial x}-B_{11}\frac{\partial^2w_0}{\partial x^2}+C_{11}\left(\frac{\partial^2w_0}{\partial x^2}-\frac{\partial\ \phi_0}{\partial x}\right)\right] \quad (34a)$$

$$M_{xx}-\mu\frac{\partial^2M_{xx}}{\partial x^2}=\left(1-\lambda\frac{\partial^2}{\partial x^2}\right)\left[B_{11}\frac{\partial u_0}{\partial x}-D_{11}\frac{\partial^2w_0}{\partial x^2}+F_{11}\left(\frac{\partial^2w_0}{\partial x^2}-\frac{\partial\ \phi_0}{\partial x}\right)\right] \quad (34b)$$

$$P_{xx}-\mu\frac{\partial^2P_{xx}}{\partial x^2}=\left(1-\lambda\frac{\partial^2}{\partial x^2}\right)\left[C_{11}\frac{\partial u_0}{\partial x}-F_{11}\frac{\partial^2w_0}{\partial x^2}+H_{11}\left(\frac{\partial^2w_0}{\partial x^2}-\frac{\partial\ \phi_0}{\partial x}\right)\right] \quad (34c)$$

$$Q_{xz}-\mu\frac{\partial^2Q_{xz}}{\partial x^2}=\left(1-\lambda\frac{\partial^2}{\partial x^2}\right)\left[A_{55}\left(\frac{\partial\ w_0}{\partial x}-\phi_0\right)\right] \quad (34d)$$

Based on the nonlocal strain gradient theory, the equilibrium equations for FG-CNTRC nanobeam can be written as

$$\begin{aligned}&\left(1-\mu\frac{\partial^2}{\partial x^2}\right)\left(A_{11}\frac{\partial^2u_0}{\partial x^2}-B_{11}\frac{\partial^3w_0}{\partial x^3}+C_{11}\left(\frac{\partial^3w_0}{\partial x^3}-\frac{\partial^2\phi_0}{\partial x^2}\right)\right)\\&=\left(1-\lambda\frac{\partial^2}{\partial x^2}\right)\left(I_0\ddot{u}_0-I_1\frac{\partial\ddot{w}_0}{\partial x}+I_3\left(\frac{\partial\ddot{w}_0}{\partial x}-\ddot{\phi}_0\right)\right)\end{aligned} \quad (35a)$$

$$\begin{aligned}&\left(1-\mu\frac{\partial^2}{\partial x^2}\right)\left(C_{11}\frac{\partial^2u_0}{\partial x^2}-F_{11}\frac{\partial^3w_0}{\partial x^3}+H_{11}\left(\frac{\partial^3w_0}{\partial x^3}-\frac{\partial^2\phi_0}{\partial x^2}\right)\right)\\&=\left(1-\lambda\frac{\partial^2}{\partial x^2}\right)\left(I_3\ddot{u}_0-I_4\frac{\partial\ddot{w}_0}{\partial x}+I_5\left(\frac{\partial\ddot{w}_0}{\partial x}-\ddot{\phi}_0\right)\right)\end{aligned} \quad (35b)$$

$$\left(1-\mu\frac{\partial^2}{\partial x^2}\right)\begin{pmatrix}C_{11}\frac{\partial^3u_0}{\partial x^3}-F_{11}\frac{\partial^4w_0}{\partial x^4}+H_{11}\left(\frac{\partial^4w_0}{\partial x^4}-\frac{\partial^3\phi_0}{\partial x^3}\right)-B_{11}\frac{\partial^3u_0}{\partial x^3}\\+D_{11}\frac{\partial^4w_0}{\partial x^4}-F_{11}\left(\frac{\partial^4w_0}{\partial x^4}-\frac{\partial^3\phi_0}{\partial x^3}\right)-A_{55}\left(\frac{\partial^2w_0}{\partial x^2}-\frac{\partial\phi_0}{\partial x}\right)\end{pmatrix}$$

$$= \left(1 - \lambda \frac{\partial^2}{\partial x^2}\right)\left(I_0 \ddot{w}_0 + I_1 \frac{\partial \ddot{u}_0}{\partial x} - I_2 \frac{\partial^2 w_0}{\partial x^2} - I_3 \frac{\partial \ddot{u}_0}{\partial x} - I_4 \left(\frac{\partial \ddot{\phi}_0}{\partial x} - 2\frac{\partial^2 \ddot{w}_0}{\partial x^2}\right) - I_5 \left(\frac{\partial^2 \ddot{w}_0}{\partial x^2} - \frac{\partial \ddot{\phi}_0}{\partial x}\right)\right) \quad (35c)$$

5. Exact solutions for FG-CNTRC nanobeams

Functions of the displacements field that satisfy the simply-simply cross-ply beams boundary conditions are developed as Fourier series as

$$\begin{aligned} u_0(x,t) &= U_m e^{i\omega t}\cos(\beta x) \\ w_0(x,t) &= W_m e^{i\omega t}\sin(\beta x) \\ \phi_0(x,t) &= X_m e^{i\omega t}\cos(\beta x) \end{aligned} \quad (36)$$

In which $i = \sqrt{-1}$, U_m, W_m and X_m are arbitrary parameters and $\beta = m\pi/L$. Substituting Eq. (35) into Eq. (36) give

$$\left((1+\lambda\beta^2)\begin{bmatrix} s_{11} & s_{12} & s_{13} \\ s_{12} & s_{22} & s_{23} \\ s_{13} & s_{23} & s_{33} \end{bmatrix} - (1+\mu\beta^2)\omega^2 \begin{bmatrix} m_{11} & m_{12} & m_{13} \\ m_{12} & m_{22} & m_{23} \\ m_{13} & m_{23} & m_{33} \end{bmatrix}\right) = \begin{Bmatrix} 0 \\ 0 \\ 0 \end{Bmatrix} \quad (37)$$

where the matrix elements of Eq. (37) can be written as

$$\begin{aligned} s_{11} = -A_{11}\beta^2,\ s_{12} = C_{11}\beta^2,\ s_{13} = C_{11}\beta^2 \\ s_{22} = D_{11}\beta^2,\ s_{23} = -F_{11}\beta^3,\ s_{33} = -H_{11}\beta^3 - A_{55}\beta^3 \end{aligned} \quad (38)$$

And

$$\begin{aligned} m_{11} = -I_0,\ m_{12} = I_3, m_{13} = I_1\beta - I_3\beta, m_{22} = I_5, \\ m_{23} = I_4\beta - I_5\beta, m_{33} = I_0 + 2I_2\beta^2 + I_5\beta^2 \end{aligned} \quad (39)$$

6. Numerical results

In the current research, numerical results are presented to illustrate the stresses and deflections of CNTRC beams using a new hyperbolic higher-order shear deformation beam theory. Also, the boundary conditions considered are simply supported. The materials chosen as reinforcement in this study are Poly methyl methacrylate (PMMA) (matrix)and the armchair (10,10) SWCNTs.

Material properties of the matrix are $\nu^p = 0.3$, $\rho^p = 1190$ Kg/m^3 and $E^p = 2.5$ GPa , and for the reinforcement $\nu^{cnt} = 0.19$, $\rho^{cnt} = 1400$ Kg/m^3 , $E_{11}^{cnt} = 600$ GPa , $E_{22}^{cnt} = 10$ GPa and $G_{12}^{cnt} = 17.2$ GPa.

Numerical results are presented in terms of non-dimensional parameters as

$$\text{For vibration analysis} \quad \overline{\omega} = \omega L\sqrt{\frac{I_{00}}{A_{110}}} \quad (40)$$

where A_{110} and I_{00} are A_{11} and I_0 of beam made of pure matrix material, respectively.

Due to the existing limitation of similar work results for multilayered CNTRC nanobeams, the validation processes of the present model for its efficiency and precision are divided into two stages: (1) a comparison study to validate the accuracy of the proposed hyperbolic shape function

Table 2 Comparison of dimensionless frequency of simply supported various kinds of CNTs distribution (L/h=15, $V_{cnt}^{*} = 0.12$)

Theory	UD	FG-O	FG-X	FG-V
FSDT[(a)] [(a)] [27]	0.9976	0.7628	1.1485	0.8592
TSDT[(a)] [27]	0.9745	0.7453	1.1152	0.8441
ESDT[(a)] [27]	0.9756	0.7440	1.1180	0.8448
HSDT[(a)] [27]	0.9745	0.7454	1.1151	0.8441
TrSDT[(a)] [27]	0.9749	0.7446	1.1163	0.8443
Present	0.9749	0.7446	1.1162	0.8443

[(a)] Wattanasakulpong and Ungbhakorn (2013)

Table 3 Effect of CNTs volume fraction and thickness ratio on the dimensionless frequencies (L/h=10)

V_{cnt}^{*}	a/h	UD	FG-X	FG-O	FG-V	FG(A)	FG(B)
12%	5	1.6497	1.7332	1.4270	1.5678	1.3429	1.7376
	10	1.2594	1.3916	1.0066	1.1272	0.9224	1.4092
	20	0.7809	0.9128	0.5827	0.6649	0.5242	0.9352
	30	0.5490	0.6545	0.4014	0.4606	0.3594	0.6737
17%	5	2.1023	2.2000	1.8189	1.9848	1.7073	2.2041
	10	1.5700	1.6711	1.2447	1.3921	1.1357	1.7607
	20	0.9530	1.1171	0.7062	0.8057	0.6332	1.1452
	30	0.6656	0.7951	0.4839	0.5552	0.4320	0.8186
28%	5	2.3427	2.3858	2.1215	2.2456	2.0159	2.3806
	10	1.8279	1.9636	1.5036	1.6464	1.3815	1.9786
	20	1.1608	1.3363	0.8731	0.9875	0.7838	1.3648
	30	0.8227	0.9726	0.6020	0.6874	0.5371	0.9990

model and (2) parametric study to investigate the effects of several parameters independently.

To examine the effectiveness of the proposed theory on the vibration behaviour of FG beams, Table 2 presents a comparative analysis by considering the existing CNTs patterns in the literature (UD, FG-X, FG-O, FG-V). The proposed results are concluded with results obtained by Wattanasakulpong and Ungbhakorn (2013) using the first-order shear deformation theory FSDT, Exponential shear deformation theory (ESDT), Third order shear deformation theory (TSDT), Hyperbolic shear deformation theory (HSDT), and Trigonometric shear deformation theory (TrSDT). Consequently, our results are identical to those generated by using the TrSDT.

Table 3 presents the effect of CNTs volume fraction and thickness ratio on the dimensionless frequencies. It is seen that the dimensionless frequencies increase by the increasing of CNTs volume fraction and decreasing the thickness ratio, regardless of the CNTs distribution pattern.

Table 4 presents the effect of nonlocal and length scale parameters on the dimensionless frequencies. It is seen that the dimensionless frequencies increase by the increasing λ and decreasing of μ, regardless of the CNTs distribution pattern.

From Fig. 2, it is observed that the proposed functionally graded materials (FG(A) and FG(B)) have an excellent and smooth variation of the distribution of the constituents, unlike the FG-X and the FG-V which have an abrupt change of distribution at the mid-plane position.

Table 4 Effect of nonlocal and length scale parameters on the dimensionless frequencies (L/h=10)

μ	λ	UD	FG-X	FG-O	FG-V	FG(A)	FG(B)
0	0	1.2594	1.3916	1.0066	1.1272	0.9224	1.4092
	0,5	1.2901	1.4255	1.0311	1.1547	0.9449	1.4435
	1	1.3200	1.4587	1.0551	1.1816	0.9669	1.4771
	1,5	1.3494	1.4911	1.0785	1.2078	0.9884	1.5099
	2	1.3781	1.5228	1.1015	1.2335	1.0094	1.5420
0,5	0	1.2294	1.3585	0.9826	1.1004	0.9005	1.3756
	0,5	1.2594	1.3916	1.0066	1.1272	0.9224	1.4092
	1	1.2886	1.4239	1.0300	1.1534	0.9439	1.4419
	1,5	1.3172	1.4556	1.0529	1.1791	0.9649	1.4740
	2	1.3453	1.4865	1.0753	1.2041	0.9854	1.5053
1	0	1.2015	1.3276	0.9603	1.0754	0.8800	1.3444
	0,5	1.2307	1.3600	0.9837	1.1016	0.9015	1.3772
	1	1.2594	1.3916	1.0066	1.1272	0.9224	1.4092
	1,5	1.2873	1.4225	1.0290	1.1523	0.9429	1.4405
	2	1.3147	1.4528	1.0508	1.1768	0.9630	1.4711
1,5	0	1.1754	1.2988	0.9395	1.0521	0.8609	1.3152
	0,5	1.2040	1.3304	0.9624	1.0777	0.8819	1.3472
	1	1.2320	1.3614	0.9847	1.1027	0.9024	1.3786
	1,5	1.2594	1.3916	1.0066	1.1272	0.9224	1.4092
	2	1.2861	1.4212	1.0280	1.1512	0.9421	1.4391
2	0	1.1509	1.2717	0.9199	1.0301	0.8430	1.2878
	0,5	1.1789	1.3027	0.9423	1.0553	0.8635	1.3192
	1	1.2063	1.3330	0.9642	1.0798	0.8836	1.3499
	1,5	1.2331	1.3626	0.9856	1.1038	0.9032	1.3798
	2	1.2594	1.3916	1.0066	1.1272	0.9224	1.4092

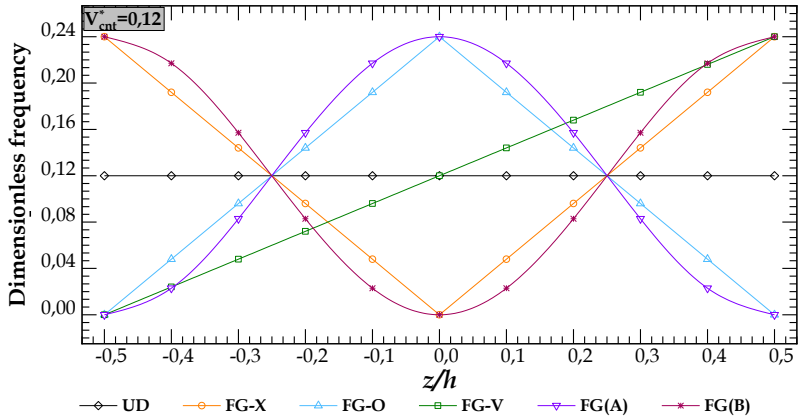

Fig. 2 Various functionally graded CNTs distribution patterns

In Fig. 3, the increase of the geometric parameter L/h decreases the dimensionless frequency $\overline{\omega}$, wherever the CNTs distribution pattern is. The FG CNTRC (B) has the highest values of

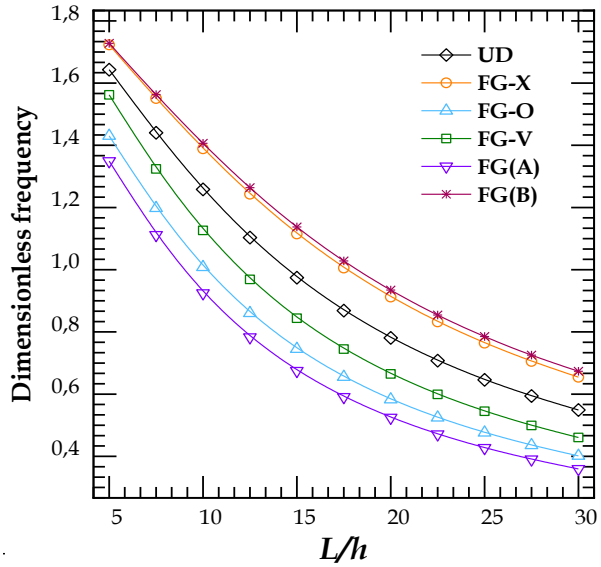

Fig. 3 Effect of thickness ratio on the dimensionless frequency $\left(V_{cnt}^{*} = 0.12, \mu = 0, \lambda = 0\right)$

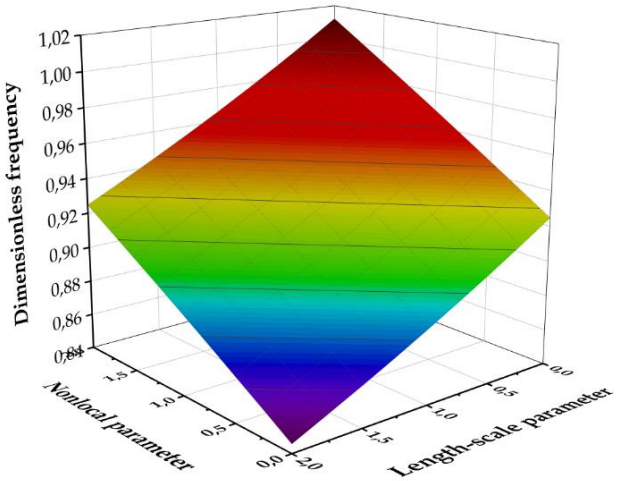

Fig. 4 Effect of nonlocal and lenght-scale parameters on the dimensionless frequency of CNTRC(A) beam

dimensionless frequency $\overline{\omega}$, while the lowest values are the CNTRC (A).

In Figs. 4 and 5, we present the action of the nonlocal and the length-scale parameters on the FG CNTRC (A) and FG CNTRC (B), respectively. The augmentation of nonlocal parameters leads to an increment in the dimensionless frequencies$\overline{\omega}$, wherever the distribution pattern is. Unlike the effect of nonlocal parameters, the augmentation of length-scale parameters leads to a decrement in dimensionless frequencies $\overline{\omega}$.

Figs. 6 and 7 plotted the effect of the mode shape m and the volume fraction of the CNTs V_{cnt}^{*} on the dimensionless frequency $\overline{\omega}$. Therefore, It is clear that the increment of the modes m and n, also leads to the increment of the dimensionless frequency $\overline{\omega}$. On the other hand, the highest

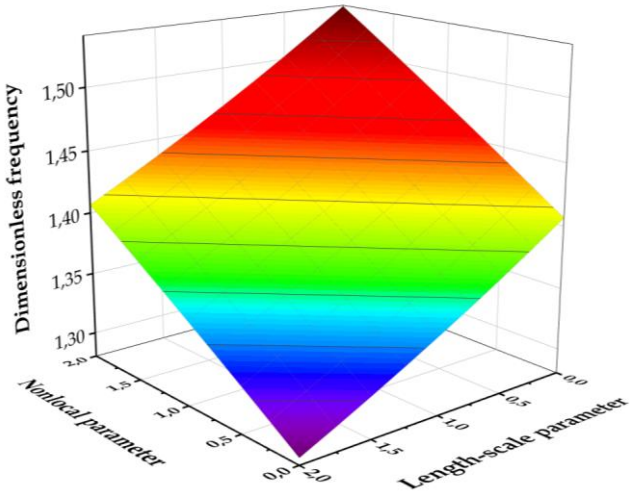

Fig. 5 Effect of nonlocal and lenght-scale parameters on the dimensionless frequency of CNTRC(B) beam

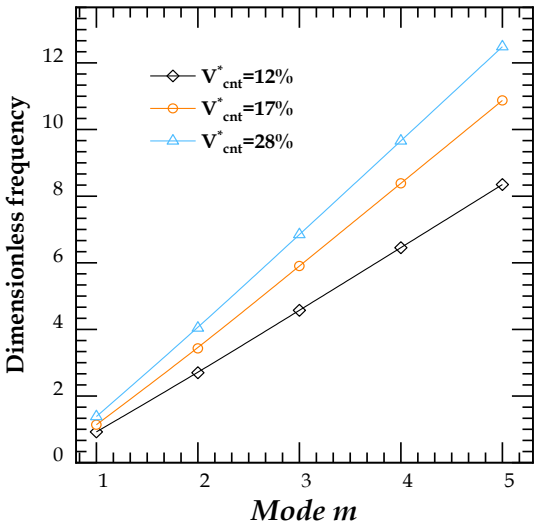

Fig. 6 Effect of mode number on the dimensionless frequency of CNTRC(A) beam

frequencies are for the beam that has a volume fraction $V_{cnt}^{*} = 0.28$, whereas the lowest values are the volume fraction $V_{cnt}^{*} = 0.12$.

7. Conclusions

The current work presents the free vibration problem of simply supported CNTRC beams reinforced by different patterns of CNT distributions in the polymeric matrix. Cosine functions describe the material gradation and material properties through the thickness. Based on the higher-order nonlocal strain gradient theory, the equilibrium equations are obtained using the virtual work

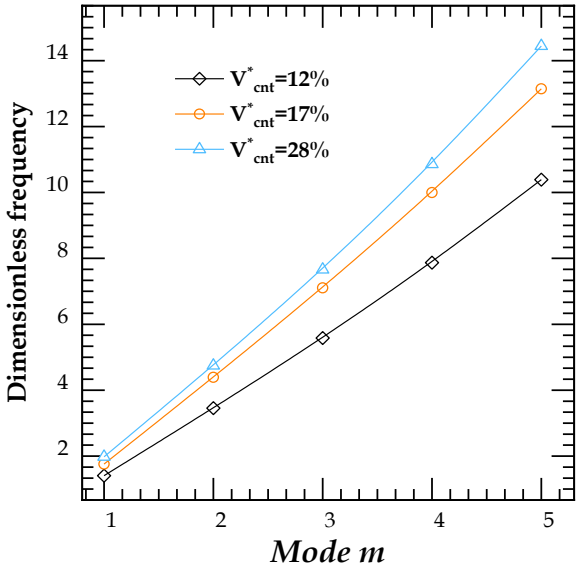

Fig. 7 Effect of mode number on the dimensionless frequency of CNTRC(B) beam

principle and solved using Navier's procedure. The accuracy of the mathematical models is numerically verified by comparison with some available results. The numerical examples show that:

- The proposed form of CNT FG-(B) has the highest rigidity, therefore, the highest frequencies. The lowest rigidity and frequencies are for the FG-(A) CNT-reinforced composite beams.
- The action of the nonlocal and the length-scale parameters on the FG CNTRC (A) and FG CNTRC (B), respectively, the augmentation of nonlocal parameter leads to an increment in the dimensionless frequencies $\overline{\omega}$, wherever the distribution pattern is. Unlike the effect of nonlocal parameters, the augmentation of length-scale parameters leads to a decrement in dimensionless frequencies $\overline{\omega}$.
- The effect of the mode shape m, n, and the volume fraction of the CNTs V_{cnt}^{*} on the dimensionless frequency $\overline{\omega}$. Consequently, It is clear that the increment of the modes m and n, also leads to the increment of the dimensionless frequency. However, the highest frequencies are for the beam with a volume fraction $V_{cnt}^{*} = 0.28$; the lowest values are the volume fraction $V_{cnt}^{*} = 0.12$.

The effect of CNTs volume fraction and thickness ratio on the dimensionless frequencies, it is seen that the dimensionless frequencies increase with the increment of CNTs volume fraction and decrement of the thickness ratio, regardless of the CNTs distribution pattern. The effect of nonlocal and length scale parameters on the dimensionless frequencies $\overline{\omega}$ is seen as the dimensionless frequencies increase through the increment of λ and decrement of μ, regardless of the CNTs distribution pattern.

References

Abdelrahman, A.A., Esen, I., Daikh, A.A. and Eltaher, M.A. (2021), "Dynamic analysis of FG nanobeam

reinforced by carbon nanotubes and resting on elastic foundation under moving load", *Mech. Bas. Des. Struct. Mach.*, 1-24. https://doi.org/10.1080/15397734.2021.1999263.

Alazwari, M.A., Esen, I., Abdelrahman, A.A., Abdraboh, A.M. and Eltaher, M.A. (2022), "Dynamic analysis of functionally graded (FG) nonlocal strain gradient nanobeams under thermo-magnetic fields and moving load", *Adv. Nano Res.*, **12**(3), 231-251. https://doi.org/10.12989/anr.2022.12.3.231.

Babaei, H., Kiani, Y. and Eslami, M.R. (2021a), "Vibrational behavior of thermally pre-/post-buckled FG-CNTRC beams on a nonlinear elastic foundation: a two-step perturbation technique", *Acta Mechanica*, **232**(10), 3897-3915. https://doi.org/10.1007/s00707-021-03027-z.

Babaei, H., Kiani, Y. and Eslami, M.R. (2021b), "perturbation method for thermal post-buckling analysis of shear deformable FG-CNTRC beams with different boundary conditions", *Int. J. Struct. Stab. Dyn.*, **21**(13), 2150175. https://doi.org/10.1142/S0219455421501753.

Bachiri, A., Daikh, A.A. and Tounsi, A. (2022), "On the thermo-elastic response of FG-CNTRC cross-ply laminated plates under temperature loading using a new HSDT", *J. Appl. Comput. Mech.*, **8**(4), 1370-1386. https://doi.org/10.22055/jacm.2022.40148.3529.

Bessaim, A., Houari, M.S.A., Bernard, F. and Tounsi, A. (2015), "A nonlocal quasi-3D trigonometric plate model for free vibration behaviour of micro/nanoscale plates", *Struct. Eng. Mech.*, **56**(2), 223-240. https://doi.org/10.12989/sem.2015.56.2.223.

Daikh, A.A., Drai, A., Houari, M.S.A. and Eltaher, M.A. (2020), "Static analysis of multilayer nonlocal strain gradient nanobeam reinforced by carbon nanotubes", *Steel Compos. Struct.*, **36**(6), 643-656. http://dx.doi.org/10.12989/scs.2020.36.6.643.

Daikh, A.A., Houari, M.S.A., Belarbi, M.O., Mohamed, S.A. and Eltaher, M.A. (2022), "Static and dynamic stability responses of multilayer functionally graded carbon nanotubes reinforced composite nanoplates via quasi 3D nonlocal strain gradient theory", *Def. Technol.*, **18**(10), 1778-1809. https://doi.org/10.1016/j.dt.2021.09.011.

El-Ashmawy, A.M. and Xu, Y. (2021), "Combined effect of carbon nanotubes distribution and orientation on functionally graded nanocomposite beams using finite element analysis", *Mater. Res. Expr.*, **8**(1), 015012. https://doi.org/10.1088/2053-1591/abc773.

Eringen, A.C. (1983), "On differential equations of nonlocal elasticity and solutions of screw dislocation and surface waves", *J. Appl. Phys.*, **54**(9), 4703-4710. https://doi.org/10.1063/1.332803.

Esen, I. (2020), "Dynamics of size-dependant Timoshenko micro beams subjected to moving loads", *Int. J. Mech. Sci.*, **175**, 105501. https://doi.org/10.1016/j.ijmecsci.2020.105501.

Esen, I. and Özmen, R. (2022a), "Free and forced thermomechanical vibration and buckling responses of functionally graded magneto-electro-elastic porous nanoplates", *Mech. Bas. Des. Struct. Mach.*, 1-38. https://doi.org/10.11-38.080/15397734.2022.2152045.

Esen, I. and Özmen, R. (2022b), "Thermal vibration and buckling of magneto-electro-elastic functionally graded porous nanoplates using nonlocal strain gradient elasticity", *Compos. Struct.*, **296**, 115878. https://doi.org/10.1016/j.compstruct.2022.115878.

Esen, I., Alazwari, M.A., Eltaher, MA. and Abdelrahman, A.A. (2022), "Dynamic response of FG porous nanobeams subjected to thermal and magnetic fields under moving load", *Steel Compos. Struct.*, **42**(6), 805-826. https://doi.org/10.12989/scs.2022.42.6.805.

Esen, I., Eltaher, M.A. and Abdelrahman, A. (2021), "Vibration response of symmetric and sigmoid functionally graded beam rested on elastic foundation under moving point mass", *Mech. Bas. Des. Struct. Mach.*, **51**(5), 2607-2631. https://doi.org/10.1080/15397734.2021.1904255.

Garg, A., Chalak, H.D., Belarbi, M.O., Zenkour, A.M. and Sahoo, R. (2021), "Estimation of carbon nanotubes and their applications as reinforcing composite materials-an engineering review", *Compos. Struct.*, **272**, 114234. https://doi.org/10.1016/j.compstruct.2021.114234.

Garg, A., Chalak, H.D., Zenkour, A.M., Belarbi, M.O. and Sahoo, R. (2022), "Bending and free vibration analysis of symmetric and unsymmetric functionally graded CNT reinforced sandwich beams containing softcore", *Thin Wall. Struct.*, **170**, 108626. https://doi.org/10.1016/j.tws.2021.108626.

Houari, M.S.A., Bessaim, A., Bernard, F., Tounsi, A. and Mahmoud, S.R. (2018), "Buckling analysis of new quasi-3D FG nanobeams based on nonlocal strain gradient elasticity theory and variable length scale

parameter", *Steel Compos. Struct.*, **28**(1), 13-24. https://doi.org/10.12989/scs.2018.28.1.013.
Jam, J.E. and Kiani, Y. (2015), "Low velocity impact response of functionally graded carbon nanotube reinforced composite beams in thermal environment", *Compos. Struct.*, **132**, 35-43. https://doi.org/10.1016/j.compstruct.2015.04.045.
Jedari Salami, S. (2018), "Free vibration analysis of sandwich beams with carbon nanotube reinforced face sheets based on extended high-order sandwich panel theory", *J. Sandw. Struct. Mater.*, **20**(2), 219-248. https://doi.org/10.1177/1099636216649788.
Keleshteri, M.M., Asadi, H. and Aghdam, M.M. (2019), "Nonlinear bending analysis of FG-CNTRC annular plates with variable thickness on elastic foundation", *Thin Wall. Struct.*, **135**, 453-462. https://doi.org/10.1016/j.tws.2018.11.020.
Keshtegar, B., Kolahchi, R., Eyvazian, A. and Trung, N.T. (2020), "Dynamic stability analysis in hybrid nanocomposite polymer beams reinforced by carbon fibers and carbon nanotubes", *Polym.*, **13**(1), 106. https://doi.org/10.1080/15376494.2011.581412.
Khelifa, Z., Hadji, L., Daouadji, T.H. and Bourada, M. (2018), "Buckling response with stretching effect of carbon nanotube-reinforced composite beams resting on elastic foundation", *Struct. Eng. Mech.*, **67**(2), 125-130. http://doi.org/10.12989/sem.2018.67.2.125.
Khosravi, S., Arvin, H. and Kiani, Y. (2019a), "Interactive thermal and inertial buckling of rotating temperature-dependent FG-CNT reinforced composite beams", *Compos.: Part B*, **175**, 107178. https://doi.org/10.1016/j.compositesb.2019.107178.
Khosravi, S., Arvin, H. and Kiani, Y. (2019b), "Vibration analysis of rotating composite beams reinforced with carbon nanotubes in thermal environment", *Int. J. Mech. Sci.*, **164**, 105187. https://doi.org/10.1016/j.ijmecsci.2019.105187.
Kiani, Y. (2016), "Thermal postbuckling of temperature-dependent sandwich beams with carbon nanotube-reinforced face sheets", *J. Therm. Stress.*, **39**(9), 1098-1110. https://doi.org/10.1080/01495739.2016.1192856.
Kiani, Y. and Mirzaei, M. (2019), "Nonlinear stability of sandwich beams with carbon nanotube reinforced faces on elastic foundation under thermal loading", *Proc. Inst. Mech. Eng.*, *Part C: J. Mech. Eng. Sci.*, **233**(5), 1701-1712. https://doi.org/10.1177/0954406218772613.
Liew, K.M., Lei, Z.X. and Zhang, L.W. (2015), "Mechanical analysis of functionally graded carbon nanotube reinforced composites: A review", *Compos. Struct.*, **120**, 90-97. https://doi.org/10.1016/j.compstruct.2014.09.041.
Lim, C.W., Zhang, G. and Reddy, J. (2015), "A higher-order nonlocal elasticity and strain gradient theory and its applications in wave propagation", *J. Mech. Phys. Solid.*, **78**, 298-313. https://doi.org/10.1016/j.jmps.2015.02.001.
Lin, F. and Xiang, Y. (2014), "Numerical analysis on nonlinear free vibration of carbon nanotube reinforced composite beams", *Int. J. Struct. Stab. Dyn.*, **14**(01), 1350056. https://doi.org/10.1142/S0219455413500569.
Lin, F. and Xiang, Y. (2014), "Vibration of carbon nanotube reinforced composite beams based on the first and third order beam theories", *Appl. Math. Model.*, **38**(15-16), 3741-3754. https://doi.org/10.1016/j.apm.2014.02.008.
Mayandi, K. and Jeyaraj, P. (2015), "Bending, buckling and free vibration characteristics of FG-CNT-reinforced polymer composite beam under non-uniform thermal load", *Proc. Inst. Mech. Eng.*, *Part L: J. Mater.: Des. Appl.*, **229**(1), 13-28. https://doi.org/10.1177/1464420713493720.
Merzouki, T., Houari, M.S.A., Bessaim, A., Haboussi, M., Dimitri, R. and Tornabene, F. (2022), "Bending analysis of functionally graded porous nanocomposite beams based on a non-local strain gradient theory", *Math. Mech. Solid.*, **27**(1), 66-92. https://doi.org/10.1177/10812865211011759.
Mirzaei, M. and Kiani, Y, (2016), "Nonlinear free vibration of temperature-dependent sandwich beams with carbon nanotube-reinforced face sheets", *Acta Mechanica*, **227**, 1869-1884. https://doi.org/10.1007/s00707-016-1593-6.
Mirzaei, M. and Kiani, Y. (2015), "Snap-through phenomenon in a thermally postbuckled temperature dependent sandwich beam with FG-CNTRC face sheets", *Compos. Struct.*, **134**, 1004-1013.

https://doi.org/10.1016/j.compstruct.2015.09.003.

Mohseni, A. and Shakouri, M. (2019), "Vibration and stability analysis of functionally graded CNT-reinforced composite beams with variable thickness on elastic foundation", *Proc. Inst. Mech. Eng., Part L: J. Mater.: Des. Appl.*, **233**(12), 2478-2489. https://doi.org/10.1177/1464420719866222.

Özmen, R., Kılıç, R. and Esen, I. (2022), "Thermomechanical vibration and buckling response of nonlocal strain gradient porous FG nanobeams subjected to magnetic and thermal fields", *Mech. Adv. Mater. Struct.*, 1-20. https://doi.org/10.1080/15376494.2022.2124000.

Salami, S.J. (2016), "Extended high order sandwich panel theory for bending analysis of sandwich beams with carbon nanotube reinforced face sheets", *Physica E: Low Dimens. Syst. Nanostr.*, **76**, 187-197. https://doi.org/10.1016/j.physe.2015.10.015.

Talebizadehsardari, P., Eyvazian, A., Asmael, M., Karami, B., Shahsavari, D. and Mahani, R.B. (2020), "Static bending analysis of functionally graded polymer composite curved beams reinforced with carbon nanotubes", *Thin Wall. Struct.*, **157**, 107139. https://doi.org/10.1016/j.tws.2020.107139.

Wang, Q., Pang, F., Qin, B. and Liang, Q. (2018), "A unified formulation for free vibration of functionally graded carbon nanotube reinforced composite spherical panels and shells of revolution with general elastic restraints by means of the Rayleigh-Ritz method", *Polym. Compos.*, **39**(S2), E924-E944. https://doi.org/10.1016/j.compstruc.2009.07.009.

Wattanasakulpong, N. and Ungbhakorn, V. (2013), "Analytical solutions for bending, buckling and vibration responses of carbon nanotube-reinforced composite beams resting on elastic foundation", *Comput. Mater. Sci.*, **71**, 201-208. https://doi.org/10.1016/j.commatsci.2013.01.028.

Yas, M.H. and Samadi, N. (2012), "Free vibrations and buckling analysis of carbon nanotube-reinforced composite Timoshenko beams on elastic foundation", *Int. J. Press. Ves. Pip.*, **98**, 119-128. https://doi.org/10.1016/j.ijpvp.2012.07.012.

Zghal, S., Frikha, A. and Dammak, F. (2020), "Large deflection response-based geometrical nonlinearity of nanocomposite structures reinforced with carbon nanotubes", *Appl. Math. Mech.*, **41**, 1227-1250. https://doi.org/10.1007/s10483-020-2633-9.

Zhu, P., Lei, Z.X. and Liew, K.M. (2012), "Static and free vibration analyses of carbon nanotube-reinforced composite plates using finite element method with first order shear deformation plate theory", *Compos. Struct.*, **94**(4), 1450-1460. https://doi.org/10.1016/j.compstruct.2011.11.010.

CC